e-ISSN:2321-6212
p-ISSN:2347-2278
RESEARCH AND REVIEWS: JOURNAL OF MATERIAL SCIENCES

Thermal Effect Behavior of Materials under Scanning Electron Microscopy. Monte Carlo and Molecular Dynamics Hybrid Model.

Abdelkader Nouiri*

Material Sciences Department, University Oum El-Bouaghi, Oum EL-Bouaghi, 04000, Algeria.

Research Article

Received: 22/08/2014
Revised: 13/09/2014
Accepted: 22/09/2014

*For Correspondence

Material Sciences Department, University Oum El-Bouaghi, Oum EL-Bouaghi, 04000, Algeria.

Keywords: Scanning electron microscope; Thermal effect of electron beam; Monte Carlo calculation; Dynamic molecular simulation

ABSTRACT

A scanning electron microscope (SEM) provides a convenient way to provide structural information at micro and nano scale. However, the temperature rise due to electron bombardment during SEM analysis has been a concern because it can modify SEM results, in particular at nanostructures. For quantitative understanding of the temperature increase during the SEM analysis, a hybrid model, molecular dynamics combined with Monte Carlo method, is developed. The influence of some parameters, like accelerating voltage, primary current and scanning duration are studied. The resulting temperature profile within semiconductors materials and hypothetical apatite grains indicates a maximum temperature increase near the surface, followed by a continuous temperature reduction as a function of depth from the surface.

INTRODUCTION

A scanning electron microscope (SEM) provides one of the most popular analytical methods to describe surface morphologies and chemical compositions of a wide range of solid materials. In many fields of material Sciences, it became a routine procedure to examine natural samples using a SEM in various modes of SE (secondary electrons), BSE (back- scattered electrons), EDS (energy dispersive spectroscopy), CL (cathodoluminescence) or EBSD (electron back-scatter diffraction). In all cases, the researchers assume that low injection condition is satisfied in SEM analysis, so the temperature rise (thermal effect) at the irradiated area is very small and is neglected. However, in reality the irradiated area is heated under the electron beam, and therefore the results obtained from the techniques associated with SEM must be rectified in particular in the nanostructures which have small dimensions near of that of interaction volume. Some old empirical expressions have been proposed [1], but their predictions are not similar and the temperature rise is not treated as a function of depth.

During the SEM analysis, incident electrons interact with atomic electrons in the sample, delivering a certain amount of kinetic energy to the sample. Most of this kinetic energy is transformed to heat in the sample, giving rise to temperature increase during the operation process [2,3] (Talmon and Thomas, 1977, 1978). Previous studies based on simulation of atomic interactions [4,5] (Mirkarimi et al., 2002; Randolph et al., 2005) or direct measurement of thermal status of samples [6,7] (Chu et al., 2002, 2003) support that the temperature increase during electron bombardment is proportional to current density. A number of models have been proposed to predict the temperature increase in samples during electron-beam exposure, but the results are widely different depending on input parameters such as conceptual model, initial condition and sample geometry. Talmon and Thomas (1977)[2] developed a numerical model to estimate the electron-beam heating problem on 2-D thin film specimens. In their study, the temperature rise is proportional to the probe current, and a temperature rise was calculated in the order of 5 K at a current density of 8 MA/m^2. Mirkarimi et al. (2002) [4] used a finite element model to study electron-beam-induced heating on a planar Mo/Si multilayer film. The calculated temperature rise is maximum (~15 K) at the center of the electron beam, and continuously decreases as a function of radial distance or depth from the sample surface. Weber (1994)[8] first employed a Monte Carlo method to simulate the energy deposition profile in the target sample. The Monte Carlo electron-solid interaction model was integrated with a finite element model by Randolph et al. (2005)[5] to determine the magnitude of electron-beam-induced heating (EBIH) on a nanofiber tip and a SiO_2 thin film (500 nm thick) as a function of current beam energy and sample geometry. For a constant probe current of 500 pA, the surface temperature decreases gradually with beam energy (maximum 30 KeV) from an initial maximum temperature of 304 K to ambient temperature. Egerton et al. (2004)[9] performed 3-D modeling for thick samples suggesting that the temperature rise is less significant than

proposed in the previous studies. For example, the temperature rise is <0.1 K for metals, and only a few degrees for a typical polymer at beam energy of 20 KV and probe current of 1 nA. Nouiri et al. (2006)[10] proposed a new Monte Carlo approach based on electron-matter interaction model, and calculated the temperature rise in semiconductors during SEM analysis. The temperature rise is proportional to the level of absorbed current and inversely related to the accelerating energy, yielding 0.3 to 20 K for an absorbed current range of 0.1 to 1 nA at the frequently used beam energy of 20 KeV. Experimental evidence of electron-beam induced temperature rise was first reported by Chu et al. (2002, 2003)[6,7]. They used nanothermocouples to measure the *on-site* temperature rise during electron-beam exposure. At the same accelerating energy (15 KV), they obtained a 70 K increase at the bottom surface of a silicon substrate (at a current density of 50 KA/m^2), a 62 K on quartz substrates (16 KA/ m^2) and a 18 K on silicon substrates (16 KA/ m^2).

Although a new Monte Carlo model was proposed to calculate the temperature rise at semiconductor material (GaAs) under an electron beam[10], but in that model, the influence on scanning duration was not taken into account. In this paper, a combination between Monte Carlo and molecular dynamics methods has been used. Therefore, a hybrid model is developed. Thanks to this model, the thermal effect of SEM can be calculated for different parameters such as the scanning duration. In addition, this model can be used to study different materials. Some first results are published for apatite [11].

Calculation procedures

The electron-matter interaction during SEM analysis may result in a range of effects on incident electrons, which can be mainly divided into two types of electron scattering: elastic and inelastic (Egerton et al., 2004)[9]. Among these effects, only one category of inelastic scattering, i.e. the excitation of lattice oscillations, is expected to be the origin of phonons leading to a substantial loss of beam energy as heating effect in the sample. To calculate the temperature rise in our case, a numerical simulation under similar SEM operating conditions is developed using a hybrid method, Monte Carlo and molecular dynamic

Because a condensed sample material is used in this simulation, several processes need to be considered to estimate temperature increase caused by the electron-matter interaction during SEM analysis [10]. Here we are interested in the excitation of lattice oscillations causing generation of phonons, therefore a substantial portion of the beam energy is transferred to the sample in the form of heat. The simulation was performed in the following steps: (1) defining numerous random pathways of the incident electrons in the sample over the entire period of entrance to exit within the material, (2) dividing the sample into several zones (Fig. 1), (3) estimating the number of phonons (Δ_{ph}) generated within each zone based on the conditions of the incident electron beam (accelerating voltage, primary current and scanning time), (4) converting the phonon excess (Δ_{ph}) into temperature rise based on thermodynamic laws, and (5) estimating conductive heat loss to correct the calculated temperature rise. More detailed calculation procedures are explained in the following sections.

Diffusion of electrons (random walk)

The phonon excess (Δ_{ph}) is generated during the collision of the incident electron with the atoms of apatite units of the target material via random walk process. After each collision, the electron loses a certain amount of energy (E_{moy}) generating one phonon (Fig. 2).

The step distance S is written as:

$$S = -\lambda \ln(R) \qquad (1)$$

where R is a random number between 0 and 1, representing the random walk model [10].

The mean free path λ in the equation (1) can be obtained from the total scattering cross section:

$$\lambda = \frac{A}{N_A \rho \sigma} \qquad (2)$$

where A is the atomic weight, N_A is the Avogadro's number, ρ is the density of the material, and σ is the total scattering cross section [10].

Scattering mechanisms can be divided into elastic and inelastic. The elastic scattering of electrons by the nuclei of the atoms, which are partially screened by the bound electrons, can be analyzed by using the Rutherford model. The total relativistic Rutherford scattering cross section can be expressed as:

$$\sigma = (5.21.10^{-21})\left[\frac{Z}{E}\right]^2\left[\frac{E + m_0c^2}{E + 2m_0c^2}\right]^2 . \frac{4\pi}{\delta(\delta+1)} \qquad (3)$$

e-ISSN:2321-6212
p-ISSN:2347-2278

where *Z* is the atomic number of the scattering unit, *E* is the energy of electron in KeV, *C* is the speed of light, m_0 is the mass of electron, and δ is a screening parameter [10].

The screening parameter δ is given by [10]:

$$\delta = \left(3.4.10^{-3}\right)\frac{Z^{0.67}}{E} \quad (4)$$

The angle for a particular scattering event can be obtained from the probability distribution:

$$\cos(\theta) = 1 - \frac{2\delta R}{1+\delta-R} \quad (5)$$

R is a random number between 0 and 1. The elastic or inelastic scattering depends on □

Calculation of the electrons depth

A spherical coordinates are used to calculate the electron paths inside of the material. After each collision, the electron changes its position with a distance of S according to the equation (1), and two alternative angles of α (0-180°) and β (0-360°):

$$\alpha = \pi.R \quad \text{and} \quad \beta = 2\pi.R$$

R is a random number between 0 and 1, therefore the Cartesian coordinates of an electron can be expressed as: (6)

$$x_i = \sum_{j=1}^{m} S_j.\sin\alpha_j.\cos\beta_j\,,\; y_i = \sum_{j=1}^{m} S_j.\sin\alpha_j.\sin\beta_j\,, z_i = \sum_{j=1}^{m} S_j.\cos\alpha_j \quad (7)$$

when *m* represents the number of steps (collisions) inside the material (from the surface until the electron energy)

In the SEM experience, an electron beam is used which corresponds to *N* electrons, the average distances projected to x, y, and z coordinates (*Sx, Sy, Sz*) for these electrons is calculated as:

$$Sx = \left[\sum_{i=1}^{N} x_i\right]/N\,,\; Sy = \left[\sum_{i=1}^{N} y_i\right]/N\,, \quad (8)$$

The maximum depth R_e is calculates as:

$$R_e = \sqrt{Sx^2 + Sy^2 + Sz^2} \qquad Zs = \left[\sum_{i=1}^{N} z_i\right]/N \quad (9)$$

In order to compare the maximum depth with other models, our calculation is extended to three models; Kanaya-Okayama, Wittry-Kyser and Everhart-Hoff [12-14]:

$$R_e(\mu m) = \left(\frac{25.6}{\rho}\right)\left(\frac{E_0}{30}\right)^{1.7} \quad \text{(Wittry-Kyser 1967)[12]} \quad (10)$$

$$R_e(\mu m) = \left(\frac{0.0398}{\rho}\right)(E_0)^{1.75} \quad \text{(Everhart-Holf 1971)[13]} \quad (11)$$

$$R_e(\mu m) = \left(\frac{0.0276A}{\rho Z^{0.889}}\right)(E_0)^{1.67} \quad \text{(Kanaya-Okayama 1972)[14]} \quad (12)$$

Calculation of the temperature rise

In this model, the temperature is considered as "room temperature", so the phonon-defect and phonon-phonon interaction are neglected. After each collision, the electron produces one phonon through excitation of lattice oscillations. According to Einstein model, the energy loss

e-ISSN:2321-6212
p-ISSN:2347-2278

as a phonon is calculated from the average thermal energy of atom Emoy:

$$E_{moy} = \left(\frac{3}{2}\right) K_B T \quad (13)$$

where K_B is the Boltzman constant. For T=300 K (room temperature), E_{moy}=38.8 meV.

At the end of the electron trajectory, the total number of generated phonons (Δ_{ph}) at each zone (Fig.1) can be calculated. The phonon energy excess (ΔQ_i) per unit of volume (e.g., cubic centimeter) is calculated as:

$$\Delta Q_i = \frac{E_{moy} \cdot \Delta_{ph(V_i)}}{V_i} \quad (14)$$

where V_i is the volume of zone "i".

This energy excess is transformed into a temperature rise ΔT_i (at each zone) using the following relationship:

$$\Delta T_i = \frac{\Delta Q_i}{\rho . c_p} \quad (15)$$

where ρ is the density (mass in cubic centimeter) and c_p is the specific heat.

The estimated ΔT_i needs to be corrected because of due to thermal conduction can dissipate heat to outside. The heat diffusion (heat flux) ΔH_i from zone "*i*-1" to zone "*i*" is written as:

$$\Delta H_i = k.a.\frac{(T_{i-1} - T_i)}{l} \quad (16)$$

where *k* is the thermal conductivity, *a* is the surface area of zone "*i*", *l* is the distance between the middle of zone "*i*-1" and the middle of zone "*i*". *l* is equal to the thickness of zone "*i*" because all the zones have the same thickness.

Finally, the ΔT_i can be calculated for each zone, representing the temperature distribution in the sample.

Influence of SEM analysis durations (molecular dynamics method)

In order to calculate the influence of analysis duration, we are obliged to use the dynamic molecular method. The principal idea is to calculate the speed of electron and the time after each collision inside the material. The kinetic energy E_k of an electron at the arrival on the surface of material can be calculated as:

$$E_0 = E_k = \frac{1}{2} m_0 v_0^2 \quad (17)$$

where E_0 is the initial energy, m_0 is the mass of electron and v_0 is the speed of electron at the surface.
After each collision, the speed of electron at the position "*j*" (v_j) can be calculated from the relationship:

$$v_j = \sqrt{\frac{2(E_{j-1} - E_j)}{m_0}} \quad (18)$$

where E_{j-1} and E_j represent the electron energies at "*j-1*" and "*j*" positions successively.

According to equation (1), the distance between two collisions is S_j. With an assumption that the movement between two collisions is rectilinear (with a constant speed), following relationship can be establised:

$$S_j = v_j . t_j \quad (19)$$

e-ISSN:2321-6212
p-ISSN:2347-2278

where t_j is the duration between the two collisions (j and j-1)

At the end of the electron trajectory, the total scattering time (t) is calculated as:

$$t = \sum_{j=1}^{m} t_j \qquad (20)$$

Where, m represents the number of steps inside the material.

Finally, the number of phonons (Δ_{ph}) can be estimated by multiplying it by a fraction time t_f:

$$t_f = \frac{scanning\ time}{scattering\ time} \qquad (21)$$

Therefore, the equation (14) becomes:

$$\Delta T_i = \frac{\Delta Q_i}{\rho . c_p} . t_f \qquad (22)$$

Examples of calculation (Results)

Figures 3a-3d represent the maximum penetration depth of electrons calculated for four materials, silicon, gallium arsenide, nano layers and apatite as a function of accelerating voltages and compared with previous results. The maximum electron depth is proportional to the accelerating energy for all models. Proposed calculations for both silicon and GaAs are generally consistent with those of Wittry-Kyser [12] and Kanaya-Okayama[14], whereas the calculated electron depth for apatite is consistent with those of Everhart and Holf (1971)[13] for lower energy (<15 KeV), but approach to the results of Wittry and Kyser (1967)[12] for higher energy (>15 KeV).

Figure 4 displays the temperature rise as a function of depth for two values of analysis duration (6.4 min and 25.6 min). It is clear that the temperature rise is high near the surface, then it diminishes rapidly inside the material. Another important finding is that the temperature rise is more significant for larger analysis duration (t_s).

Figure 5 shows the effects of primary current which is proportional to the number of electrons. It is apparent that more temperature rise induced by higher primary current. In contrast to commercial conductors or semiconductors, the fluorapatite has low thermal conductivity (0.0133 W cm^{-1} K^{-1}) causing only limited conductive heat loss, thus most of the thermal energy is retained within the sample.

Figure 1: Schematic diagram showing the electron-matter interaction. Solid curves display the locations used in the model simulation, whereas the color gradient represents a semi-qualitative estimates of the resulting temperature.

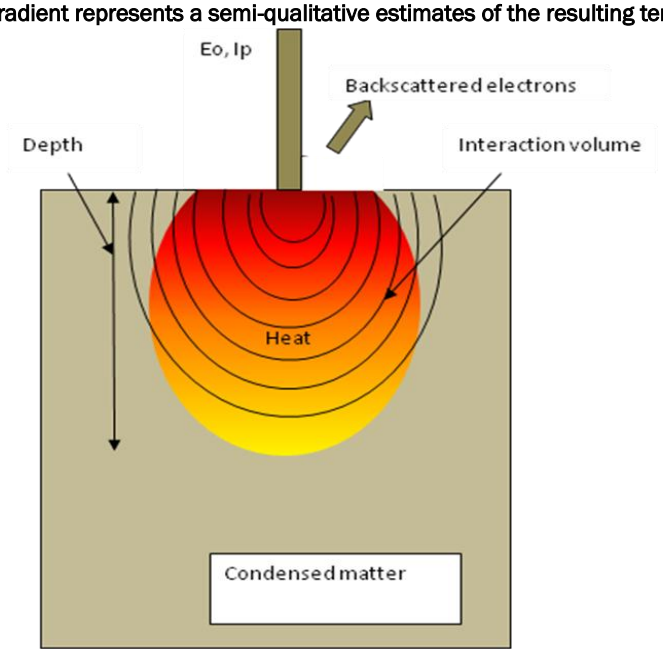

e-ISSN:2321-6212
p-ISSN:2347-2278

Figure 2: Schematic representation of the calculation procedure.

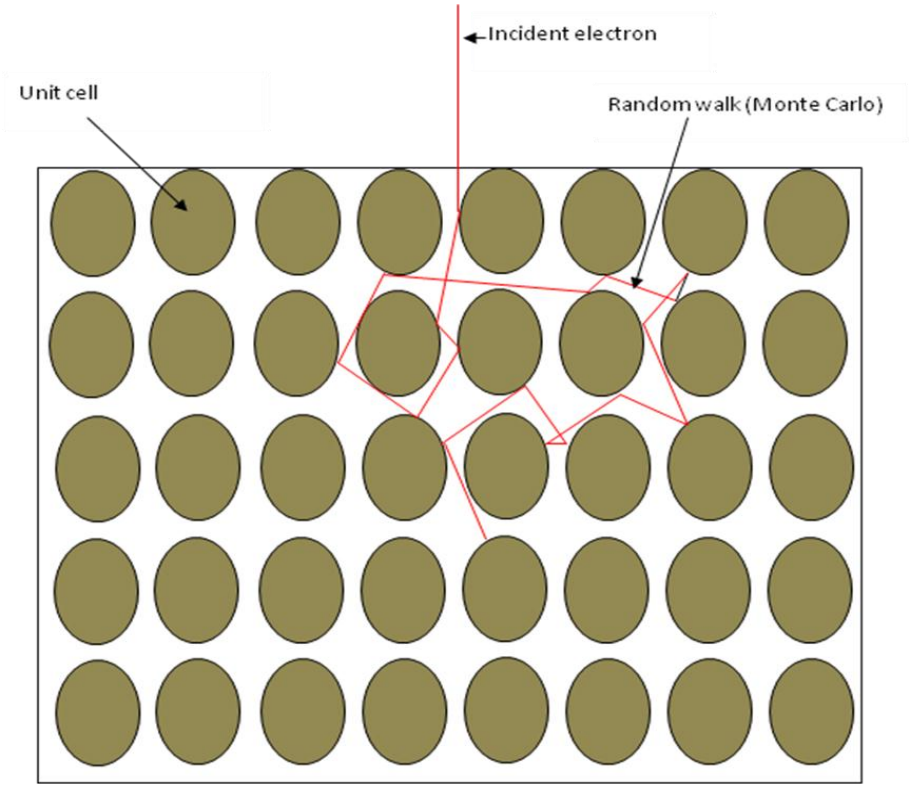

Figure 3a-3d: Depth as a function of accelerating energy for Si(a), GaAs(b), Apatite(c) and nano layers AlAs/GaAs/AlAs (d)

Figure 3a

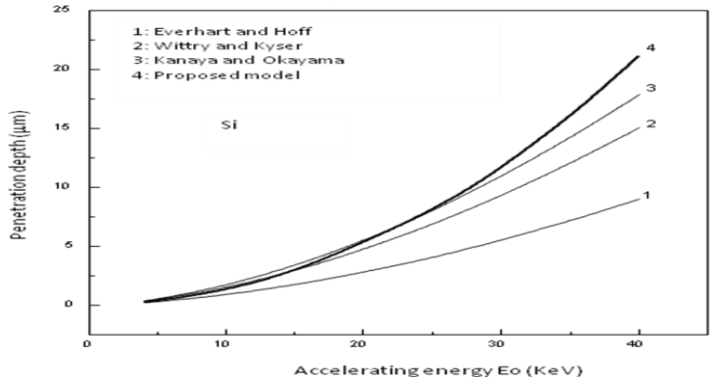

Figure 3b

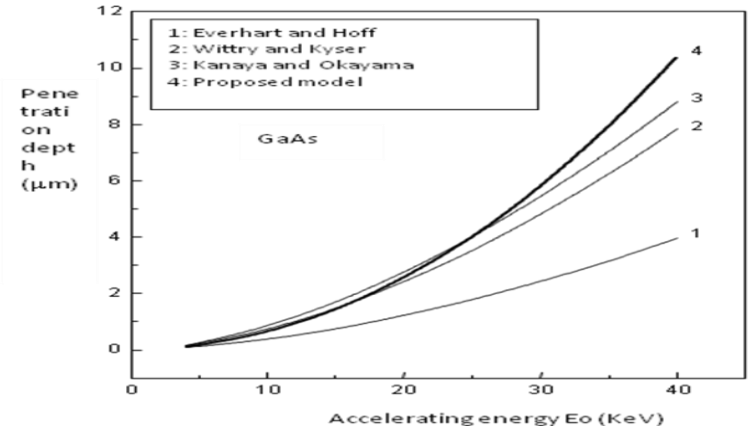

e-ISSN:2321-6212
p-ISSN:2347-2278

Figure 3c

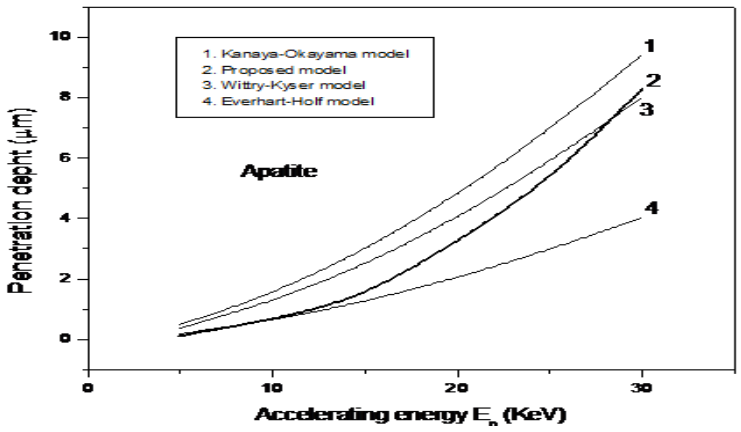

Figure 3d

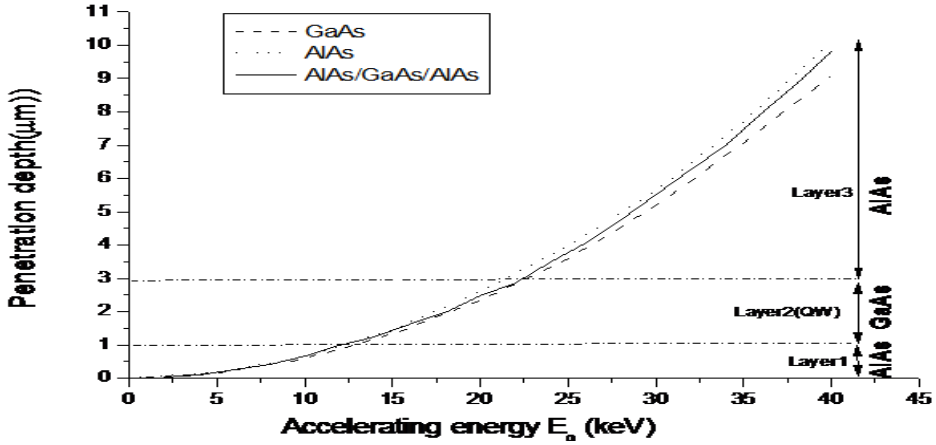

Figure 4: Temperature rise as a function of depth.

Figure 4a

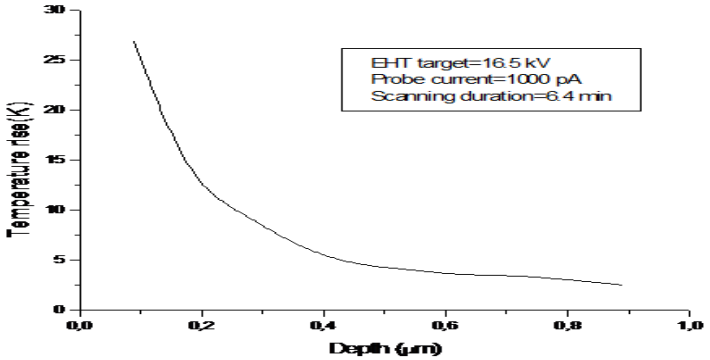

Figure 4a

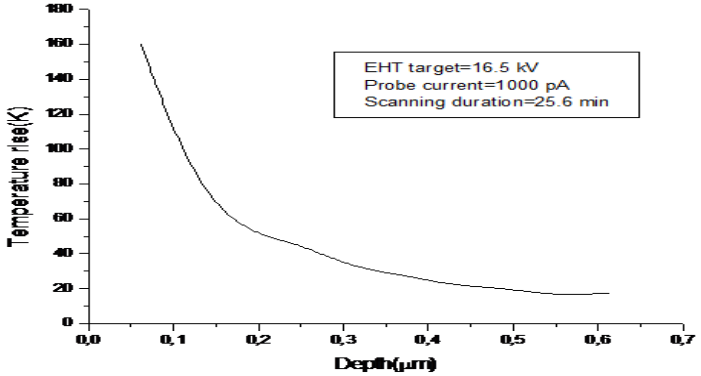

e-ISSN:2321-6212
p-ISSN:2347-2278

Figure 5: Temperature rise as a function of depth for two values of primary current.

Figure 5a

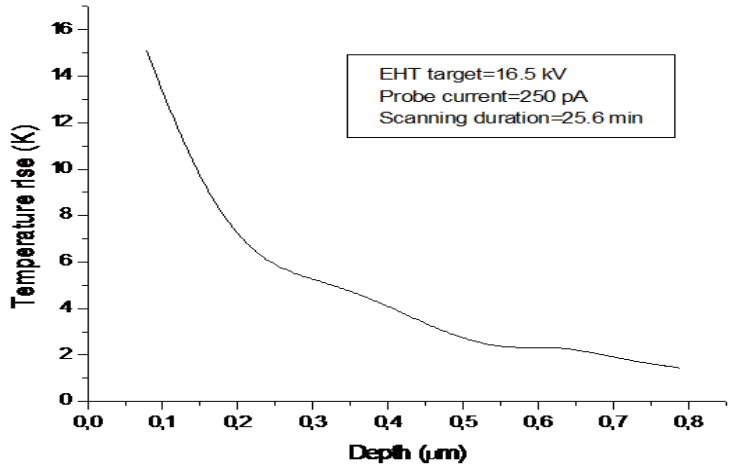

Figure 5b

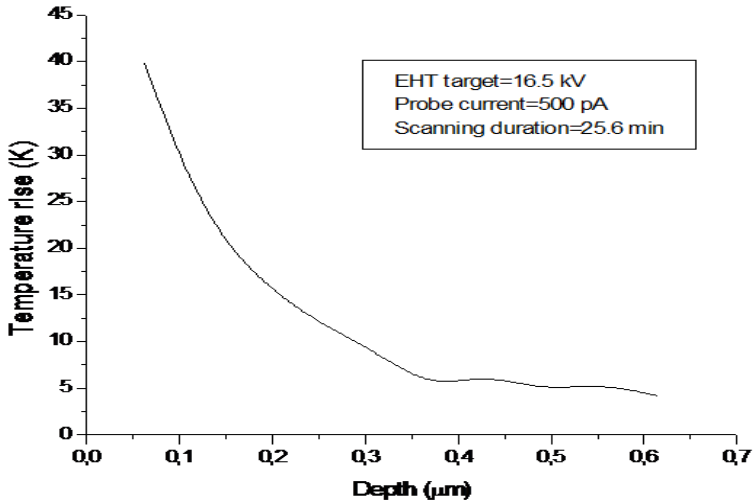

CONCLUSION

A correction term of electron beam temperature rise must be taken into account during the scanning electron analysis in order to improve the material characterization results, in particular at nano scale.

ACKNOWLEDGEMENTS

The author thanks Pr. Kyoungwon (Kyle) Min and Dr. Jingnan Shan from University of Florida (USA) for the experimental parameters of apatite

REFERENCES

1. S. Achour, Cathodoluminescence determination of the temperature rise in CdS under an electron beam spot, Philos. Mag. B 62,3 (1990)329-336
2. Y. Talmon, E.L. Thomas, Beam heating of a moderately thick cold stage specimen in the SEM/STEM, Journal of Microscopy. 111, (1977)151–164.
3. Y. Talmon, E.L. Thomas, Electron beam heating temperature profiles in moderately thick cold stage STEM/SEM specimens, Journal of Microscopy. 113, (1978)69–75.
4. P.B. Mirkarimi, D.G. Stearns, S.L. Baker, J.W. Elmer, D.W. Sweeney, E.M. Gullikson, Method for repairing Mo/Si multilayer thin film phase defects in reticles for extreme ultraviolet lithography, Journal of Applied Physics. 91, (2002)81–89.
5. S. Randolph, J. Fowlkes, P. Rack, Effects of heat generation during electronbeam-induced deposition of nanostructures, Journal of Applied Physics. 97, (2005) 124312.

6. Dachen Chu,a) D. Taner Bilir, and R. Fabian W. Pease, Submicron thermocouple measurements of electron-beam resist heating, J. Vac. Sci. Technol. B, 20, 6 (2002)
7. Dachen Chu, Wai-Kin Wong, Kenneth E. Goodson, R. Fabian W. Pease,Transient temperature measurements of resist heating using nanothermocouples, J. Vac. Sci. Technol. B 21, (2003)2985
8. M. Weber, Scattering of non-relativistic electrons in tip structures, J. Phys. D: Appl. Phys. 27 (1994)1363
9. R. Egerton, P. Li, M. Malac, Radiation damage in the TEM and SEM, Micron 35, (2004)399–409.
10. A. Nouiri, S. Chaguetmi and N. Belabed, Monte Carlo model of the temperature rise at a GaAs surface under an electron beam, Surf. Interface. Anal., 38, (2006)1153-1157
11. J. Shan, K. Min, A. Nouiri, Thermal effects of Scanning Electron Microscopy on He diffusion in apatite: Implications for (U-Th)/He dating, Chemical Geology, 345, (2013)113-118.
12. D.B. Wittry, D.F. Kyser, Measurement of diffusion lengths in direct-gap semiconductors by electron-beam excitation, Journal of Applied Physics 38, (1967)375–382.
13. T. Everhart, P. Hoff, Determination of kilovolt electron energy dissipation vs penetration distance in solid materials, Journal of Applied Physics 42, (1971)5837–5846.
14. K. Kanaya and S. Okayma, Penetration and energy-loss theory of electrons in solid targets. J. Phys. D: Appl. Phys. 5, (1972)43